

# Density-functional studies of the electronic structure of the perovskite oxides: $\text{La}_{1-x}\text{Ca}_x\text{MnO}_3$

S. Satpathy

*Department of Physics and Astronomy, University of Missouri, Columbia, Missouri 65211*

Zoran S. Popović and Filip R. Vukajlović

*Laboratory for Theoretical Physics, Institute of Nuclear Sciences- "Vinča", 11001 Belgrade, Yugoslavia*

Using density-functional methods, we study the electronic structures of the lanthanum-based "double-exchange" perovskite magnets. Antiferromagnetic insulating solutions are obtained for both the end members,  $\text{LaMnO}_3$  and  $\text{CaMnO}_3$ , within the local density approximation (LDA), with the Jahn-Teller (JT) distortion of the oxygen octahedron taken into account. The JT distortion splits off the  $\text{Mn}(3d)e_g$  bands producing an energy gap within the LDA, with the bands derived from the  $(z^2-1)$  orbital, pointed along the long basal-plane Mn—O bond, occupied and the  $(x^2-y^2)$  bands empty. The on-site Coulomb repulsion and the intra-site exchange terms are found to be, respectively,  $U \approx 8-10$  eV and  $J \approx 0.9$  eV, from the "constrained" density-functional theory. The large value of  $U$  as compared to the bandwidth indicates that the manganese perovskite oxides are strongly correlated systems. © 1996 American Institute of Physics. [S0021-8979(96)49208-8]

The hole-doped manganese perovskite oxides, such as  $\text{La}_{1-x}\text{Ca}_x\text{MnO}_3$ , are prime examples of solids with a ferromagnetic conducting state caused by the "double exchange" mechanism, where the magnetic coupling between localized spins on neighboring atoms is mediated via conduction electrons.<sup>1-4</sup> Both the end-members,  $\text{LaMnO}_3$  and  $\text{CaMnO}_3$ , are antiferromagnetic (AF) insulators with, respectively,  $\text{Mn}^{3+}$  ( $t_{2g}^3e_g^1$ ) and  $\text{Mn}^{4+}$  ( $t_{2g}^3e_g^0$ ) configurations of the Mn ions. The localized spins of the  $t_{2g}$  electrons are coupled ferromagnetically by the doped holes in the partially filled  $e_g$  band introduced by the Ca atoms. Thus, the partially filled  $e_g$  band is responsible simultaneously for ferromagnetism and conduction in the solid. This is precisely what is experimentally observed, viz., that the mixed valence compound  $\text{La}_{1-x}\text{Ca}_x\text{MnO}_3$  shows the highest electrical conductivity for  $0.2 \leq x \leq 0.4$ , exactly in the concentration range where the material is ferromagnetic.<sup>5</sup> New interest on these systems has been revived by the recent discovery of colossal magnetoresistance (CMR) in the La-Ca-Mn-O films.<sup>6,7</sup>

In this paper, we examine the electronic structure of the two end members,  $\text{LaMnO}_3$  and  $\text{CaMnO}_3$ , from density-functional band calculations using the local spin-density approximation (LDA), as well as the "constrained" density-functional and the "LDA+U" theories.<sup>8</sup>

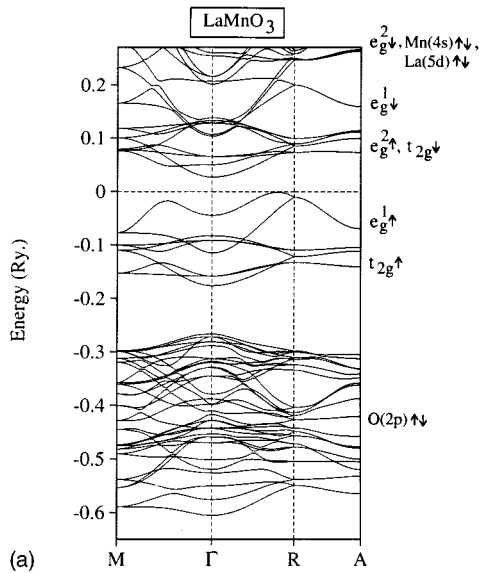
Both  $\text{LaMnO}_3$  and  $\text{CaMnO}_3$  form in the orthorhombic crystal structure<sup>9</sup> which is a distorted form of the cubic perovskite structure. While in the Ca compound, the distortion of the O octahedra surrounding the manganese atoms is largely absent, in the La compound, the octahedra are distorted significantly with three distinct Mn—O bond lengths. The Jahn-Teller (JT) distortion of the O octahedron is understandable in view of the  $t_{2g}^3e_g^1$  configuration of the Mn ion. In addition to the JT distortion, there is a slight rotation of the octahedra, which is neglected in the calculations reported here. All our calculations reported here were performed using the linear muffin-tin orbitals (LMTO-ASA) method<sup>10</sup> and the ideal tetragonal crystal structure for the two perovskites

with inclusion of the JT distortions. Thus, the magnetic unit cell in our calculation has four formula units for  $\text{LaMnO}_3$  and two for  $\text{CaMnO}_3$ .

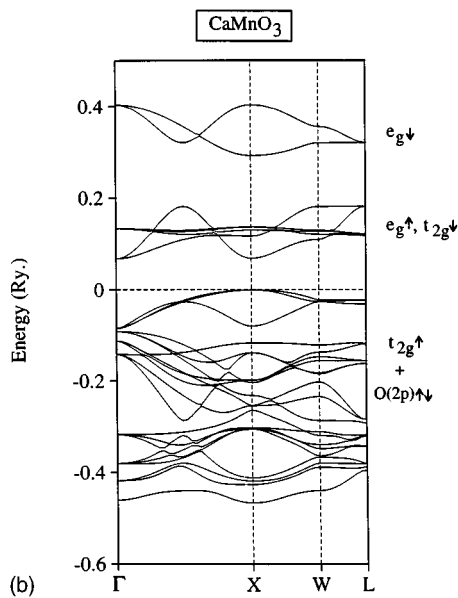
The antiferromagnetic band structures of  $\text{LaMnO}_3$  and  $\text{CaMnO}_3$  are shown in Fig. 1. The observed AF order, type A for the former and type G for the later compound,<sup>11</sup> is reproduced from the local-density calculations. The key features of the AF band structures agree with the independent LAPW calculations of Pickett and Singh.<sup>12</sup> As seen from Fig. 1, the key orbitals near  $E_f$  are the  $\text{O}(2p)$  and  $\text{Mn}(3d)$  orbitals with the energy gap occurring in the middle of the  $\text{Mn}(3d)$  bands. The outer electrons from the La, Ca, and Mn atoms are transferred to complete the  $2p$  shell of the oxygen atoms, resulting in the nominal chemical formulas of  $\text{La}^{3+}\text{Mn}^{3+}\text{O}_3^{2-}$  and  $\text{Ca}^{2+}\text{Mn}^{4+}\text{O}_3^{2-}$ , respectively.

We have studied the effect of the Jahn-Teller distortion of the cubic octahedra on the band structure by performing a series of calculations for  $\text{LaMnO}_3$  with various amounts of the distortion. There are three types of distortions<sup>13</sup> affecting the Mn—O bond lengths: (i) The breathing mode ( $Q_1$ ), (ii) the basal-plane distortion mode ( $Q_2$ ) with one diagonally opposite O pair displaced outwards and the other pair displaced inwards, and (iii) the octahedral stretching mode ( $Q_3$ ) where the four in-plane O atoms are displaced inwards and the two apical O atoms are displaced outwards. The amplitudes of these three modes in  $\text{LaMnO}_3$  are, respectively, 0.08, 0.20, and 0.11 Å, resulting in the three distinct Mn—O bond lengths: 1.91, 2.19, and 1.96 Å. We find that the basal-plane distortion mode  $Q_2$  is the most effective in splitting up the  $e_g$  bands in  $\text{LaMnO}_3$  thereby producing an energy gap, and that the  $Q_1$  or the  $Q_3$  distortions are relatively ineffective in opening up the gap. We find that a JT distortion of the  $Q_2$  type, with the oxygen atoms displaced by at least the amount  $\approx 0.1$  Å from their ideal positions, is necessary to produce a band gap in  $\text{LaMnO}_3$ . In the crystal, the measured value of this distortion is about 0.15 Å, which is therefore enough for the insulating solution. The  $t_{2g}$  bands in contrast remain more-or-less unaffected by the distortions.

The splitting of the  $\text{Mn}(3d)$  bands in  $\text{LaMnO}_3$  due to the



(a)



(b)

FIG. 1. Electronic band structures of antiferromagnetic  $\text{LaMnO}_3$  and  $\text{CaMnO}_3$  in the ideal tetragonal structure with, respectively, type A and type G magnetic configurations. The Jahn-Teller distortion of the oxygen octahedra was included for  $\text{LaMnO}_3$ . The symmetry components  $e_g$  and  $t_{2g}$  correspond to the  $\text{Mn}(3d)$  orbital, and spin components ( $\uparrow$  or  $\downarrow$ ) are local to individual atoms. Energies are with respect to  $E_f$ .

combined effects of the cubic crystal field, exchange, and the Jahn-Teller distortion as obtained from our calculations has been shown in Fig. 2. The exchange splitting is about 3.0 eV which removes the minority-spin bands up above  $E_f$ . The cubic crystal-field splitting between the  $t_{2g}$  and the  $e_g$  orbitals is about  $\Delta_{cf} \approx 2.0$  eV, while the  $Q_2$  distortion of the oxygen octahedron splits the  $e_g$  bands by  $\Delta_{JT} \approx 1.5$  eV. The total band width of the occupied  $\text{Mn}(3d)$  bands is about 2.4 eV. Of this, the  $t_{2g}$  bands are 1.3 eV wide, while the Jahn-Teller split  $e_g^1$  band just below  $E_f$  has a width of about 1.6 eV.

We find that the occupied  $\text{Mn}(e_g)$  band is derived from the  $z^2-1$  orbital, while the unoccupied band is derived from the  $x^2-y^2$  orbital, in a Mn-atom-based local coordinate sys-

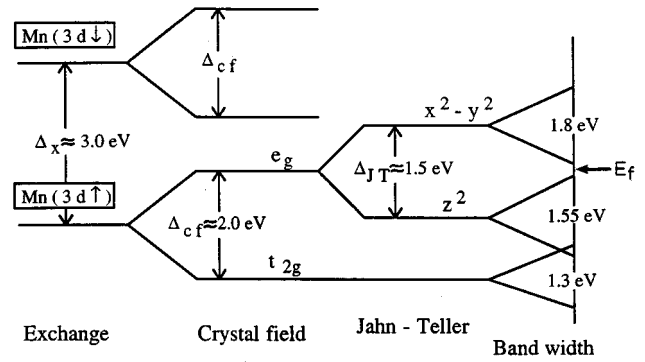


FIG. 2. Multiplet splitting of the  $\text{Mn}(3d)$  orbital for  $\text{LaMnO}_3$  as obtained from the density-functional calculation.

tem with the  $z$  axis along the long, basal-plane Mn—O bond. This is illustrated in Fig. 3, where we have shown the dominant orbital contribution<sup>14</sup> to the band structure. Occupation of the  $z^2-1$  band gives rise to the  $t_{2g}^3 e_g^1$  configuration of the Mn atom for  $\text{LaMnO}_3$ . In the mixed compound, the  $e_g^1$  band is progressively depleted with Ca concentration  $x$ , with complete depletion for the end-member  $\text{CaMnO}_3$  ( $x=1$ ).

Electron bands<sup>12,16</sup> for  $\text{LaMnO}_3$  in the experimentally observed crystal structure are not very different from the band structure shown in Fig. 1(a). Two differences may be noticed: (i) the  $\text{O}(2p)$  bands are separated from the  $\text{Mn}(3d)$  bands here, a feature that disappears for the experimental structure, and (ii) the  $e_g^1$  and the  $t_{2g}$  bands just below the  $E_f$  overlap, while for the experimental crystal structure, additional interaction results in a small separation between the  $e_g^1$  and the  $t_{2g}$  bands. In spite of this separation, however, the

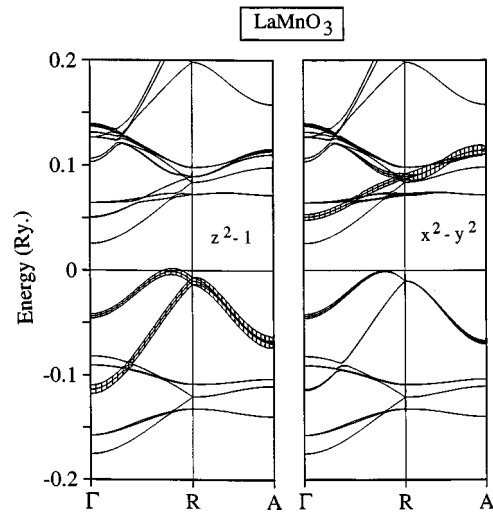


FIG. 3. Contribution of the  $\text{Mn}(3d)z^2-1$  and  $x^2-y^2$  orbitals, to the band structure. The orbitals are with respect to a Mn-atom-based local coordinate system with the  $z$  axis pointing towards a long Mn—O bond on the basal plane. The width of each band in the figure shown by cross hatching, is proportional to the contribution of the  $3d$  orbital ( $z^2-1$  or  $x^2-y^2$ ) on a specific Mn atom.

TABLE I. Energy  $\bar{\epsilon}_d$  of the central site Mn(3d) level (in Rydberg) for two different values of the “constrained” occupancy  $n_d$  for the case of LaMnO<sub>3</sub>. The occupancies of the *s* and *p* electrons on the Mn site and the total valence charges on the neighboring in-plane ( $n_{O1}$ ) and out-of-plane ( $n_{O2}$ ) oxygen atoms are also shown.

$n_d$	$\bar{\epsilon}_d$	$n_s$	$n_p$	$n_{O1}$	$n_{O2}$
4.5	-0.44	0.39	0.51	6.05	6.16
5.5	0.33	0.26	0.38	5.96	6.17

excursion of the  $z^2 - 1$  character into the  $t_{2g}$  group of bands, as seen from the left panel of Fig. 3 near the  $\Gamma$  point, is nevertheless retained in the electron bands for the experimental crystal structure [see inset of Fig. 2(a) in Ref. 16].

To assess the importance of the correlation effects, we have estimated the magnitudes for the on-site Coulomb ( $U$ ) and the intra-atomic exchange ( $J$ ) parameters for the Mn atom from constrained density-functional calculations.<sup>15</sup> The Coulomb parameter  $U$  was calculated from the dependence of the on-site energy  $\bar{\epsilon}_d$  of the Mn( $d$ ) orbital on the number occupancy  $n_d$  of a central Mn site,

$$\bar{\epsilon}_d = \epsilon_d + U \times (n_d - 1), \quad (1)$$

with the interaction of the central Mn( $d$ ) orbitals with the rest of the system switched off. This procedure is somewhat different from the one we reported earlier,<sup>16</sup> where we employed a Slater’s transition rule for the calculation of  $U$ , but we get very similar results in both cases. By constraining all  $d$  electrons on a central Mn site in a 4-atom supercell calculation, we obtain a value of about 10.4 eV for  $U$ .<sup>17</sup>

In Table I, we show the screening charges on the central Mn atom and the neighboring O atoms, for two different constrained values of  $n_d$ . The change in the number of 3d electrons is screened by only about 13% each by the Mn *s* and *p* electrons. The four in-plane oxygen atoms together contribute about 36% while the two out-of-plane oxygen atoms contribute a negligible 2% to the screening charge. The rest of the screening charge resides on more distant neighbors. Such relatively poor screening results in the high value for the Coulomb parameter  $U$ .

However, since the screening charges reside on the sphere centers in the LMTO calculation, while in reality such charges on neighboring atoms are displaced towards the central atom, the Coulomb interaction may be somewhat overestimated.<sup>18</sup> A lower bound for  $U$  is obtained by supposing that the screened charges on the neighboring oxygen atoms are located at the surface of the central Mn sphere, which then yields the maximum value for the error to be about 2.1 eV, with the resultant lower bound of  $U \approx 8.3$  eV. Thus, our calculations indicate a value of  $U \approx 8 - 10$  eV, which is consistent with the estimate of  $U \approx 7.5$  eV from an analysis of the photoemission data.<sup>19</sup> Such large values for  $U$  indicate significant electronic correlation. The calculated magnitude of the on-site parameter is  $J \approx 0.86$  eV, which is typical of binary transition-metal oxides, where it varies between 0.78 to 0.98 eV.<sup>8</sup>

With the calculated Coulomb and exchange parameters, we have minimized the LDA+ $U$  functional,<sup>8</sup> which takes into account the effects of the large Hubbard  $U$  term in a meanfield sense. The results discussed in detail elsewhere<sup>16</sup> show that there is a significant spectral redistribution. In particular, while in the LDA calculations, the Mn(3d) bands occur above O(2p) bands, in the LDA+ $U$  calculations in the Mn(3d) bands have shifted down in energy with respect to the O(2p) states and occur in the lower part of a joint band of about 7-eV wide, which is consistent with the valence-band photoemission data.<sup>22</sup> Even though the relative positions of the Mn(3d) and the O(2p) bands are reversed in the LDA+ $U$  results as compared to the LDA results, both results are consistent with the 7-eV-wide joint Mn(3d)—O(2p) double-peak structure seen in the valence-band photoemission.<sup>20–22</sup> A clearer experimental evidence for a large Coulomb  $U$  is indicated by the Mn(2p) core-level photoemission spectra, where a satellite peak is seen at the binding energy of  $\approx 10$  eV.<sup>19,20,23</sup>

This work was supported in part by the Office of Naval Research under Contract No. ONR N00014-95-1-0439 and by the Serbian Scientific Foundation under the project, “Physics of Condensed Matter and New Materials,” Grant No. 3.

<sup>1</sup>C. Zener, Phys. Rev. **82**, 403 (1951).

<sup>2</sup>P. W. Anderson and H. Hasegawa, Phys. Rev. **100**, 675 (1955).

<sup>3</sup>P.-G. De Gennes, Phys. Rev. **118**, 141 (1960).

<sup>4</sup>J. B. Goodenough, Phys. Rev. **100**, 564 (1955).

<sup>5</sup>G. H. Jonker and J. H. Van Santen, Physica **16**, 337 (1950); J. H. Van Santen and G. H. Jonker, Physica **16**, 599 (1950).

<sup>6</sup>R. von Helmolt, J. Wecker, B. Holzapfel, L. Schultz, and K. Samwer, Phys. Rev. Lett. **71**, 2331 (1993).

<sup>7</sup>S. Jin, T. H. Tiefel, M. McCormack, R. A. Fastnacht, R. Ramesh, and L. H. Chen, Science **264**, 413 (1994).

<sup>8</sup>V. Anisimov, J. Zaanen, and O. K. Andersen, Phys. Rev. B **44**, 943 (1991).

<sup>9</sup>J. B. A. A. Elemans, B. van Laar, K. R. van der Veen, and B. O. Loopstra, J. Solid State Chem. **3**, 238 (1971).

<sup>10</sup>O. K. Andersen, Phys. Rev. B **12**, 3060 (1975).

<sup>11</sup>E. O. Wollan and W. C. Koehler, Phys. Rev. **100**, 545 (1955).

<sup>12</sup>W. E. Pickett and D. J. Singh, Phys. Rev. B **53**, 1146 (1996).

<sup>13</sup>M. D. Sturge, *Solid State Physics*, edited by F. Seitz, D. Turnbull, and H. Ehrenreich (Academic, New York, 1967), Vol. 20.

<sup>14</sup>O. Jepsen and O. K. Andersen, Z. Phys. B **97**, 35 (1995).

<sup>15</sup>P. H. Dederichs, S. Blügel, R. Zeller, and H. Akai, Phys. Rev. Lett. **53**, 2512 (1984); A. K. McMahan, R. M. Martin, and S. Satpathy, Phys. Rev. B **38**, 6650 (1988).

<sup>16</sup>S. Satpathy, Z. S. Popović, and F. R. Vukajlović, Phys. Rev. Lett. **76**, 960 (1996).

<sup>17</sup>Instead, if we constrain only the number of  $e_g$  electrons on the central Mn atom, allowing the rest of the electrons including the central site  $t_{2g}$  electrons to screen the interaction, we get the value of  $U \approx 8.5$  eV.

<sup>18</sup>V. Drchal, O. Gunnarsson, and O. Jepsen, Phys. Rev. B **44**, 3518 (1991).

<sup>19</sup>A. E. Bocquet, T. Mizokawa, T. Saitoh, H. Namatame, and A. Fujimori, Phys. Rev. **46**, 3771 (1992).

<sup>20</sup>A. Chainani, M. Mathew, and D. D. Sharma, Phys. Rev. B **47**, 15 397 (1993).

<sup>21</sup>J. Zhang, D. N. McIlroy, P. A. Dowben, S. H. Liou, R. F. Sabirianov, and S. S. Jaswal, Solid State Commun. **97**, 39 (1996).

<sup>22</sup>R. P. Vasquez (unpublished).

<sup>23</sup>M. Abbate *et al.*, Phys. Rev. B **46**, 4511 (1992).